Adaptive and Robust Sliding Mode Position Control of IPMSM Drives

Mohamed ZAKY[1,2*], Shaban SHABAN[1,3], Tamer FETOUH[1,2]
[1]*Department of Electrical Engineering, Northern Border University, Arar,1321, Saudi Arabia*
[2]*Department of Electrical Engineering, Minoufiya University, Shebin El-Kom, 32511, Egypt*
[3]*Department of Basic Science, Minoufiya University, Shebin El-Kom, 32511, Egypt*
[*]*mszaky78@yahoo.com*

***Abstract*—This paper proposes an adaptive and robust sliding mode control (SMC) for the position control of Interior Permanent Magnet Synchronous Motor (IPMSM) drives. A switching surface of SMC is designed using a Linear Quadratic Regulator (LQR) technique to simultaneously control the tracking trajectory and load torque changes. The quadratic optimal control method is used to select the state feedback control gain that constitutes the system dynamic performance under uncertainties and disturbances. Feedback and switching gains are selected to satisfy both stability and fast convergence of the IPMSM. Matlab/Simulink is used to build the drive system. Experimental implementation of the IPMSM drive is carried out using DSP-DS1102 control board. The efficacy of the proposed position control method is validated using theoretical analysis and simulation and experimental results.**

***Index Terms*—adaptive sliding mode control, interior permanent magnet synchronous motor, linear quadratic regulator, position control.**

I. INTRODUCTION

Interior Permanent Magnet Synchronous Motors (IPMSMs) have been utilized growingly for industrial motor drives [1]. In past decades, Field-Oriented Control (FOC) has been considered one of the widely popular techniques for high performance applications of AC motors [2]. It has made AC motors possess torque-generating capability like DC ones by decoupling the torque and flux control variables of an IPMSM. Although many control strategies have been proposed to make the tuning of FOC for obtaining better decoupling characteristics, the ideal decoupling is still limited due to load changes and parameter variations [3-4]. If the motor parameters set in FOC scheme cannot be tuned according to their real values, the torque will become sluggish and oscillatory. Therefore, many research works have been made on the control methods of IPMSM to keep a high-performance that possesses rapid response, robustness to parameters variation and disturbances.

Position control of electrical drives is utilized in applications like conveyor belts, robotic systems, servo drives [5]. Conventionally, DC motors have been employed owing to their linear behavior and excellent control performance [6]. However, the IPMSM exhibits many advantages such as low cost, high efficiency, reliability, ruggedness, and low maintenance. So, IPMSMs are highly attractive for various applications [7-8]. But, accurate position control is a difficult problem as a result of uncertainties and disturbances.

The control methods can be classified into three categories. The first category includes traditional fixed controllers [3]. Fixed gain controllers have been commonly employed in motor drives owing to their easy design and implement. However, load dynamics and parameters variation influence their desired control specifications [4, 9-10]. The second category involves adaptive controllers such as nonlinear control [11] and Sliding Mode Control (SMC) [12]. Nevertheless, these controllers rely on the system parameters which degrade their performance. In the third category, Artificial Intelligence (AI) techniques have been given a great attention in motor drives [13-17]. The main advantages of AI schemes are that they don't require the precise mathematical model of the system. But, AI control methods suffer from high computational time.

Nowadays, SMC has gained considerable attraction for controlling AC drive systems [18]. It can offer several advantages, such as rapid dynamic response and robustness to load changes and parameters mismatches [19]. In general, a conventional SMC has two design modes, namely, the reaching mode and sliding mode. In the reaching mode, the system state is pushed towards the switching surface. During this period, the system response is sensitive to parameters variation, noise, and the tracking error cannot be controlled directly. Thus, it is essential to abbreviate the period of the reaching mode. In order to reduce the sensitivity of SMC, the reaching mode should be accelerated using larger discontinuous control gains. However, this causes chattering effects and may cause instability and large switching losses [20].

The robustness property of SMC is maintained only during the sliding mode and not necessarily during the reaching mode because of the simultaneous changes of the state and the trajectories. Therefore, with a proper design of the switching surface, SMC can meet the conventional control aims such as stabilization, tracking, regulation, etc. Certainly, the conventional switching surface cannot keep the required dynamic performance during the reaching mode [21].

Several research activities to guarantee the robustness of SMC were presented in [6], [19], [22-24]. These methods minimize chattering problem. However, their switching manifold and convergence time were constant. Consequently, tuning the switching plane is of utmost importance to achieve robust and adaptive control, and then, accurate and fast dynamic response is guaranteed under uncertainties and disturbances [25-29].

The authors wish to acknowledge the approval and the support of this research study by the grant no. 4/6/1436/5 from the Deanship of Scientific Research in Northern Border University, Arar, KSA.

Digital Object Identifier 10.4316/AECE.2017.01009

From the previous literature review, the most significant objective is to design a switching plane for SMC to achieve robust and adaptive position control under parameters variation and load torque disturbances. This will improve the decoupling characteristics of FOC, reduce the duration of the reaching phase, remove the chattering problem, and guarantee good tracking and regulation responses. Therefore, the switching surface of SMC using a Linear Quadratic Regulator (LQR) technique is designed. The quadratic optimal control method is applied to calculate the gain *G* and adapts a sliding gain of SMC. A detailed simulation and experimental results under different operating conditions is offered.

II. Mathematical Models of IPMSM And Control System

A. IPMSM Model

A mathematical model for an IPMSM is expressed by [5]:

$$\frac{\mathrm{d}i_q}{dt} = -\frac{R_s}{L_q} i_q - \frac{L_d}{L_q} \omega_r i_d + \frac{1}{L_q} V_q - \frac{\lambda_m}{L_q} \omega_r \tag{1}$$

$$\frac{\mathrm{d}i_d}{dt} = -\frac{R_s}{L_d} i_d + \frac{L_q}{L_d} \omega_r i_q + \frac{1}{L_d} V_d \tag{2}$$

The motor torque is described by

$$T_e = \frac{3}{2}\frac{P}{2}\left[\lambda_m i_q^* + \left(L_d - L_q\right) i_d^* i_q^*\right] \tag{3}$$

Mechanical equation is

$$T_e = J_o \ddot{\theta}_m + B_o \dot{\theta}_m + T_L \tag{4}$$

$$\frac{d\dot{\theta}_m}{dt} = \omega_m \tag{5}$$

where, V_d, V_q are the d and q-axes stator voltages; i_d, i_q are the d and q-axes stator currents; R_s is the stator resistance; L_d, L_q are the d and q-axes stator inductances; T_e, T_L are the electromagnetic and load torques; J_o is the moment of inertia of the motor and load; B_o is the friction coefficient of the motor; P is the number of poles of the motor; λ_m is the rotor magnetic flux linkage; ω_r, ω_m are the electrical and mechanical speeds; and θ_m is the rotor mechanical position, which is related to the rotor electrical position, θ_r, by $\theta_m = \theta_r / P$.

B. FOC Model

The field-oriented control and stator current control are employed using $i_d^* = 0$. Therefore, equation (3) is rewritten by

$$T_e = K_t i_q^* \tag{6}$$

where, the torque constant K_t is defined as

$$K_t = \frac{3}{2}\frac{P}{2}\lambda_m \tag{7}$$

Using (4) and (6), one obtains

$$K_t i_q^* = J_o \ddot{\theta}_m + B_o \dot{\theta}_m + T_L \tag{8}$$

Based on the aforementioned model, the position control system of an IPMSM drive is constructed as shown in the block diagram of Fig. 1. There are two control loops. In the outer loop, the actual rotor position is compared with the reference one. Then, the position error passed through the SMC to provide the torque component. The quadrature-axis current reference, i_q^* is calculated from (6). The direct-axis current reference i_d^* is adjusted to be zero. The two reference currents (i_q^*, i_d^*) in synchronous reference frame are converted to (i_q^s, i_d^s) in the stationary reference frame using Park's axes transformation as follows:

$$\begin{bmatrix} i_d^s \\ i_q^s \end{bmatrix} = \begin{pmatrix} \cos\theta_r & \sin\theta_r \\ -\sin\theta_r & \cos\theta_r \end{pmatrix} \cdot \begin{bmatrix} i_d^* \\ i_q^* \end{bmatrix} \tag{9}$$

The two currents (i_q^s, i_d^s) are converted to the two phase current references (i_a^*, i_b^*) as expressed in (10) and the third current i_c^* is calculated from them.

$$\begin{bmatrix} i_a^* \\ i_b^* \end{bmatrix} = \begin{pmatrix} 1 & 0 \\ -1/2 & \sqrt{3}/2 \end{pmatrix} \cdot \begin{bmatrix} i_d^s \\ i_q^s \end{bmatrix} \tag{10}$$

The actual currents of the motor are compared with the reference ones and the error passed through hysteresis current controller to produce the gate pulses. The inner current control loop is implemented as shown in Fig. 2. In the hysteresis current controller, the gate pulses are obtained from the comparison of the current error with a fixed hysteresis band. The hysteresis controller logic control can be described based on the following procedures taking phase *a* as an example,

For the positive half cycle $i_a^* > 0$: $S_4 = 0$,

If $i_a > i_a^* + \Delta i$ Then $S_1 = 0$;

Else if $i_a < i_a^* - \Delta i$ Then $S_1 = 1$;

Else no change.

For the negative half cycle $i_a^* < 0$: $S_1 = 0$,

If $i_a > i_a^* + \Delta i$ Then $S_4 = 1$;

Else if $i_a < i_a^* - \Delta i$ Then $S_4 = 0$;

Else no change.

III. Sliding Mode Position Control of IPMSM

By considering uncertainties, the mathematical model of (8) is rewritten as follows

$$\ddot{\theta}_m = \left(a_o + \Delta a\right)\dot{\theta}_m + \left(b_o + \Delta b\right) i_q^* + \left(d_o + \Delta d\right) T_L \tag{11}$$

where, $a_o = -\frac{B_o}{J_o}$, $b_o = \frac{K_t}{J_o}$, and $d_o = -\frac{1}{J_o}$, and the terms Δa, Δb, and Δd represents the uncertainties of the terms a_o, b_o, and d_o respectively.

The position error is expressed by:

$$e(t) = \theta_m^*(t) - \theta_m(t) \tag{12}$$

where, $\theta_m^*(t)$ denotes the rotor position command.

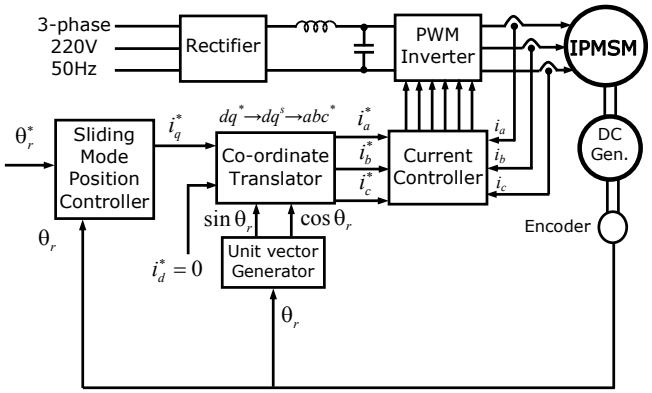

Figure 1. Block diagram for a SMC of the position controller of an IPMSM drive

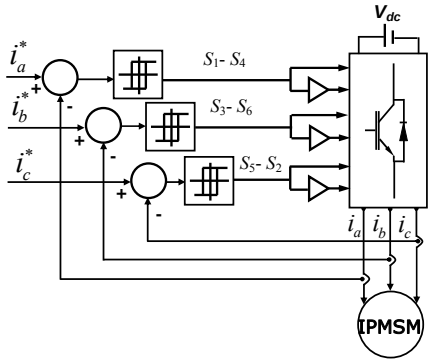

Figure 2. Inner hysteresis current control loop

Substituting from (11) in a second derivative of (12) gives

$$\ddot{e}(t) = \ddot{\theta}_m^*(t) - \ddot{\theta}_m(t) = a_o\dot{e}(t) + u(t) + d(t) \tag{13}$$

where,

$$u(t) = -b_o i_q^*(t) + \ddot{\theta}_m^*(t) - a_o\dot{\theta}_m^*(t) - d_o T_L \tag{14}$$

and

$$d(t) = -\Delta a\dot{\theta}_m(t) - \Delta d T_L - \Delta b i_q^*(t) \tag{15}$$

A. Design of Sliding Plane

A sliding plane for SMC is expressed as:

$$S(t) = \dot{e}(t) + Ge(t) = 0 \tag{16}$$

G is the positive feedback gain.

On a sliding plane (16), $S(t) = \dot{S}(t) = 0$, the error dynamics of (13) can be restricted with (17).

$$\ddot{e}(t) = -G\dot{e}(t) \tag{17}$$

As clear in (17), the error dynamics of the control system are governed by selecting the parameter G. But, constant G cannot provide the desired rapid control performance with changing the operating conditions or varying the machine parameters. Moreover, it causes that SMC is sensitive to uncertainties and disturbances, particularly during the reaching phase.

Using a proposed sliding plane, a SMC can be proposed by:

$$u(t) = -(G + a_o)\dot{e}(t) - \beta\,\mathrm{sgn}\big(S(t)\big) \tag{18}$$

where, β can be defined as a sliding coefficient, and

$$S(t) = \begin{cases} +1, & if \;\; S(t) > 0 \\ -1, & if \;\; S(t) < 0 \end{cases} \tag{19}$$

B. Selection of the Switching Gain

In SMC, a Lyapunov theory is employed to select β that minimizes the convergence rate. A Lyapunov function is chosen as follows:

$$V(t) = \frac{1}{2}S^T(t)\cdot S(t) \tag{20}$$

Its derivative can be derived as:

$$\dot{V}(t) = S(t)\dot{S}(t) = S(t)\big[\ddot{e}(t) + G\dot{e}(t)\big] \tag{21}$$

Using (13) and (18), the above equation yields

$$\begin{aligned}\dot{V}(t) &= S(t)\dot{S}(t) = S(t)\big[a_o\dot{e}(t) + u + d_o + G\dot{e}(t)\big] \\ &= S(t)\big[(G + a_o)\dot{e}(t) - (G + a_o)\dot{e}(t) - \beta\,\mathrm{sgn}(S) + d_o\big] \\ &= S(t)\big[-\beta\,\mathrm{sgn}(S) + d_o\big]\end{aligned} \tag{22}$$

For a stable control design, $\dot{V}(t)$ should be less than zero.

$$\dot{V}(t) = |S||d_o| - |\beta||S| < 0 \tag{23}$$

Then, the switching gain can be selected as:

$$|\beta| > |d_o| \tag{24}$$

The switching gain is selected as

$$\beta = d_{\max} + \eta \tag{25}$$

where η is a positive constant and $d_{\max}$ represents the maximum bound of the system uncertainties and disturbances.

The position control based on (14) and (18) can be described as

$$i_q^*(t) = \frac{1}{b_o}\begin{pmatrix}(G + a_o)\dot{e}(t) + \ddot{\theta}_m^*(t) \\ -a_o\dot{\theta}_m^*(t) - d_o T_L + \beta\,\mathrm{sgn}\big(S(t)\big)\end{pmatrix} \tag{26}$$

The most important aim of this work is to adapt G to guarantee a robust position controller under disturbances and parameters uncertainty.

To eliminate chattering of SMC, a discontinuous switching function of SMC is smoothed out by using a saturation switching function by exchanging the discontinuous switching function by a continuous one, that is

$$\mathrm{sat}\big(S\big) = \begin{cases} +1, & if \;\; S > W \\ -1, & if \;\; S < -W \\ S/L, & if \;\; |S| \le W \end{cases} \tag{27}$$

where, L is a positive number and $\pm W$ defines the thresholds of the boundary layer.

Equation (26) of continuous SMC is expressed as

$$i_q^*(t) = \frac{1}{b_o}\begin{pmatrix}(G + a_o)e(t) + \ddot{\theta}_m^*(t) \\ -a_o\dot{\theta}_m^*(t) - d_o T_L + \beta\,\mathrm{sat}\big(S(t)\big)\end{pmatrix} \tag{28}$$

IV. Adaptive Switching plane Design Using LQR

The switching plane of SMC introduced by (17) is of considerable importance to enhance the dynamic behavior of IPMSM drives. Thus, a feedback gain is designed to be tuned with changing operating conditions to give fast control. The design procedure of G using LQR method is given in the following subsections.

A. State Space Model

Denote a position error by:

$$x_1(t) = \theta_m^*(t) - \theta_m(t) \tag{29}$$

Differentiate (29) gives:

$$x_2(t) = \dot{x}_1(t) = \dot{\theta}_m^*(t) - \dot{\theta}_m(t) \tag{30}$$

Then,

$$\left.\begin{aligned} \dot{x}_2(t) &= \ddot{\theta}_m^*(t) - \ddot{\theta}_m(t) \\ &= a_o x_2(t) - b_o i_q^*(t) - d_o T_L + \ddot{\theta}_m^*(t) \\ &\quad - a_o \dot{\theta}_m^*(t) - \Delta a \dot{\theta}_m(t) - \Delta d_o T_L - \Delta b i_q^*(t) \end{aligned}\right\} \tag{31}$$

Under the assumption that the position reference, $\theta_m^*(t)$, is constant, then $\dot{\theta}_m^*(t)$, $\ddot{\theta}_m^*(t)$ can be neglected. The resultant error state equation (31) is derived as

$$\dot{x}_2(t) = \left(a_o + \Delta a\right) x_2(t) - \left(b_o + \Delta b\right) i_q^*(t) - \left(d_o + \Delta d\right) T_L \tag{32}$$

Thus, the IPMSM model can be expressed as Multiple-Input Single-Output to take into consideration the effect of external load disturbance by the following equation.

$$\left\{\begin{aligned} &\dot{x}(t) = Ax(t) + Bu(t) \\ &\begin{bmatrix} \dot{x}_1(t) \\ \dot{x}_2(t) \end{bmatrix} = \begin{bmatrix} 0 & 1 \\ 0 & a_o + \Delta a \end{bmatrix} \begin{bmatrix} x_1(t) \\ x_2(t) \end{bmatrix} \\ &\qquad + \begin{bmatrix} 0 & 0 \\ -\left(b_o + \Delta b\right) & -\left(d_o + \Delta d\right) \end{bmatrix} \begin{bmatrix} i_q^*(t) \\ T_L \end{bmatrix} \end{aligned}\right. \tag{33}$$

which is written as follows

$$\begin{bmatrix} \dot{x}_1(t) \\ \dot{x}_2(t) \end{bmatrix} = \begin{bmatrix} 0 & 1 \\ 0 & a_1 \end{bmatrix} \begin{bmatrix} x_1(t) \\ x_2(t) \end{bmatrix} + \begin{bmatrix} 0 & 0 \\ b_1 & d_1 \end{bmatrix} \begin{bmatrix} i_q^*(t) \\ T_L \end{bmatrix} \tag{34}$$

where,

$$a_1 = a_o + \Delta a,\ b_1 = -\left(b_o + \Delta b\right),\ d_1 = -\left(d_o + \Delta d\right) \tag{35}$$

B. Feedback Gain G Design

A Linear Quadratic Regulator (LQR) control technique gives a systematic approach for calculating the feedback gain *G*.

First, a state space model is written as

$$\dot{x}(t) = Ax(t) + Bu(t) \tag{36}$$

G is designed for optimal *u* by

$$u = -Gx \tag{37}$$

To reduce the performance index of (38) which expressed by

$$J_{pi} = \int_0^\infty \left(x^T Q x + u^T R u\right) dt \tag{38}$$

where Q is a positive definite matrix and R is a positive definite matrix.

The performance index J_{pi} expressed in (38) is function of the state *x(t)* and the control input *u(t). Then, if* J_{pi} *is small,* it is surely limited*, and this implies that* neither *x(t)* nor *u(t)* can be too large. This means that J_{pi} is finite, and it is an infinite integral of *x(t)*. So, *x(t)* tends to zero as *t* tends to infinity. This ensures that the closed loop control system will be *stable.*

Selection of the two parameters Q and R has a major effect on J_{pi} and hence, the system stability and performance. If the parameter Q is selected as large value, then the state *x(t)* must be smaller in order to maintain J_{pi} is small. Large value of Q reveals that the state *x(t)* decays more rapidly to zero because the poles of a closed loop system of matrix $(A - BG)$ goes further in a stable region of s-plane. Alternatively, If the parameter R is selected as large value, this means that the control input *u(t)* must be smaller to maintain J_{pi} small. Large value of R reveals that less control effort is developed, and then the poles are generally slower, and as a result larger values of the state *x(t)*. Therefore, Q is selected as a large value, whereas R is selected as a small value.

Parameter G is calculated using:

$$G = -R^{-1} B^T P \tag{39}$$

The matrix P is calculated using a Riccati equation of (40).

$$PA + A^T P - R^{-1} P B B^T P + Q = 0 \tag{40}$$

The design procedures are explained in the following steps:

1. Calculate the matrix P from (40). The system is stable when a positive-definite matrix P exists.

$$\begin{aligned} &\begin{bmatrix} P_{11} & P_{12} \\ P_{12} & P_{22} \end{bmatrix} \begin{bmatrix} 0 & 1 \\ 0 & a_1 \end{bmatrix} + \begin{bmatrix} 0 & 0 \\ 1 & a_1 \end{bmatrix} \begin{bmatrix} P_{11} & P_{12} \\ P_{12} & P_{22} \end{bmatrix} - \\ &\begin{bmatrix} 1 \end{bmatrix} \begin{bmatrix} P_{11} & P_{12} \\ P_{12} & P_{22} \end{bmatrix} \begin{bmatrix} 0 & 0 \\ b_1 & d_1 \end{bmatrix} \begin{bmatrix} 0 & b_1 \\ 0 & d_1 \end{bmatrix} \begin{bmatrix} P_{11} & P_{12} \\ P_{12} & P_{22} \end{bmatrix} \\ &+ \begin{bmatrix} q_1 & 0 \\ 0 & q_2 \end{bmatrix} = 0 \end{aligned} \tag{41}$$

Simplifying (41), gives

$$\left.\begin{aligned} &q_1 - \left(b_1^2 + d_1^2\right) P_{12}^2 = 0 \\ &P_{11} + a_1 P_{12} - \left(b_1^2 + d_1^2\right) P_{12} P_{22} = 0 \\ &2P_{12} + 2a_1 P_{22} - \left(b_1^2 + d_1^2\right) P_{22}^2 + q_2 = 0 \end{aligned}\right\} \tag{42}$$

Solving these three simultaneous equations for P_{11}, P_{12}, and P_{22}, provided that P is positive definite.

2. The matrix P is used to calculate G from (39) as:

$$G = -\begin{bmatrix} 1 \end{bmatrix} \begin{bmatrix} 0 & b_1 \\ 0 & d_1 \end{bmatrix} \begin{bmatrix} P_{11} & P_{12} \\ P_{12} & P_{22} \end{bmatrix} = -\begin{bmatrix} b_1 P_{12} & b_1 P_{22} \\ d_1 P_{12} & d_1 P_{22} \end{bmatrix} \tag{43}$$

So, the characteristic equation $\left|sI - A + BG\right| = 0$ becomes

$$s^2 - \left[a_1 + \left(b_1^2 + d_1^2\right) P_{22}\right] s - \left(b_1^2 + d_1^2\right) P_{12} = 0 \tag{44}$$

Fig. 3 illustrates the schematic block diagram of the proposed SM position controller.

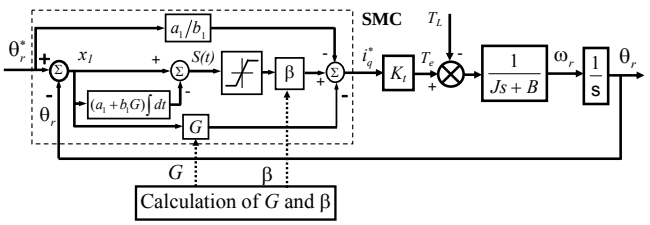

Figure 3. A schematic block diagram of a sliding mode position control method

Using the IPMSM parameters of Table I, it is found that

K_t = 2.268 Nm/A, d_{max} =15, η = 5, β = 20. The parameters Q and R are chosen as follows:

$$Q = \begin{bmatrix} 1000 & 0 \\ 0 & 10 \end{bmatrix} \qquad R = 1$$

A simple software program is built to compute the matrices P, G and the poles of the closed loop system by knowing the matrices A, B, Q and R. It is found that the matrix P is calculated as

$$P = \begin{bmatrix} 100 & 0.0008 \\ 0.0008 & 0.0001 \end{bmatrix}$$

The resultant feedback gain is $G^T = \begin{bmatrix} -31.6 & -3.1 \end{bmatrix}$. The poles of the closed loop dynamic system are at –10 and –11953, respectively.

The performance index J_{pi} is calculated using (38). If it is a small value, this ensures that the closed loop control system will be stable. Otherwise, another value of G is selected to realize the required performance.

V. Simulation Results

A. Performance under Parameters Variation

Schematic block diagram for the position control of an IPMSM drive is depicted in Fig. 1. The position controller using adaptive feedback gain of the IPMSM is shown in the block diagram of Fig. 3. To test the drive performance using the proposed adaptive SMC and the conventional SMC, simulated responses were evaluated with parameters variation ($J = J_o$ and $J = 2J_o$). Fig. 4 illustrates the effect of changing the load inertia at position reference of 10 rad. There is a similar performance using the two controllers without parameters uncertainty. However, the conventional SMC takes a larger time in case of parameters uncertainty as illustrated in Fig. 4(a). In case of the proposed adaptive SMC with variable switching gain, longer settling time is not remarkable as shown in Fig. 4(b).

Simulated speed responses with different inertias using both the adaptive and the conventional SMC are shown in Fig. 5. As observed, the proposed SMC gives superior performance than the conventional SMC. Fig. 6 shows the simulated phase plane trajectories with different inertias using both the proposed and the conventional position controllers. As observed, the proposed SMC-based IPMSM drive can track the reference position better than the conventional SMC.

B. Performance under Position Reference Tracking

The simulation results during the tracking performance under a step change of position reference using the proposed position control scheme based on adaptive sliding mode control are shown in Fig. 7 and Fig. 8. The IPMSM was operated at 2 Nm load condition. Fig. 7 shows the tracking performance under a step position reference change in forward and reverse directions with load torque of 2 Nm. The simulation results showing the tracking performance under a square wave trajectory at position reference changed from 1 to –1 rad with load torque of 2 Nm are depicted in Fig. 8. As shown, the position response tracks the reference one smoothly without overshoot and with a small rising time.

C. Performance under Ramp Speed Trajectory

Fig. 9 shows the simulation results of position and speed responses during the tracking performance under a trapezoidal position reference of 2 rad with load torque of 2 Nm. Also, Fig. 10 shows the simulation results during the tracking performance under a trapezoidal position reference of 10 rad with load torque of 2 Nm. The two figures are presented in motoring and regenerating modes of operation using the proposed position control scheme based on adaptive feedback gain. It is noted that the position error is very small in steady state. Also, the speed response precisely tracks the reference one with very small error during transients and without error during the steady state. Also, it is evident that a good position tracking is obtained without chattering phenomenon. This is because of the adaptive feedback gain. This figure is presented in comparison to [30]. As proved, the proposed method has a small position and speed errors in comparison to [30]. This confirms the validity of the proposed position control method.

D. Performance under Load Torque Disturbance

The simulation position and speed responses to justify the validity of the proposed controller under load torque disturbances are presented in Fig. 11. In this figure, the rotor position tracks the desired reference position in spite of load torque disturbances. There is a sudden load torque of 2 Nm at t = 2 sec. As shown, a small position error can be noted at this time t = 2 sec. However, the rotor position error is removed after a short time because of the adaptive feedback gain. It is observed that a good load torque rejection is achieved. This confirms that the proposed SM position control scheme works properly.

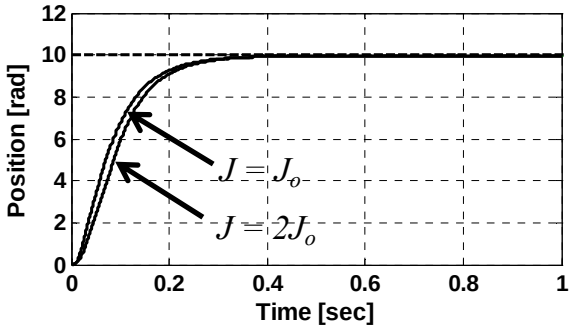

(a)

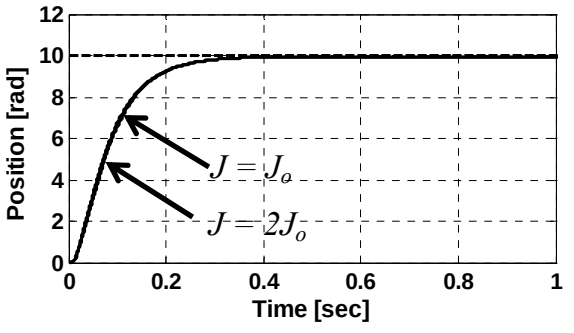

(b)

Figure 4. Simulated position responses with different inertias: a) Traditional SMC, b) Proposed SMC

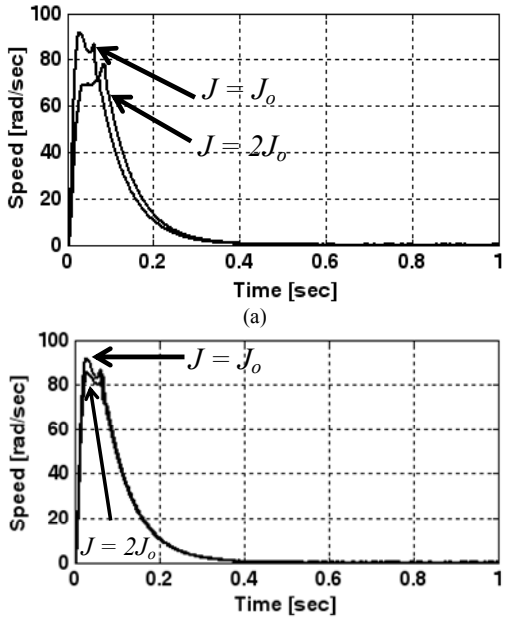

Figure 5. Simulated speed responses with different inertias: a) Traditional SMC, b) Proposed SMC

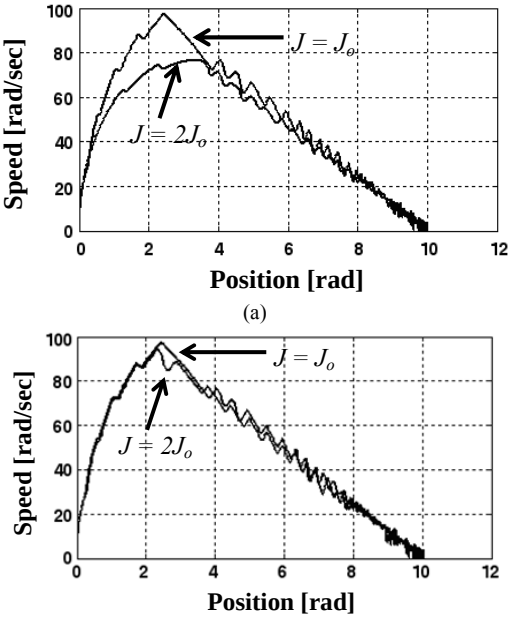

Figure 6. Simulated phase plane trajectories with different inertias: a) Traditional SMC, b) Proposed SMC

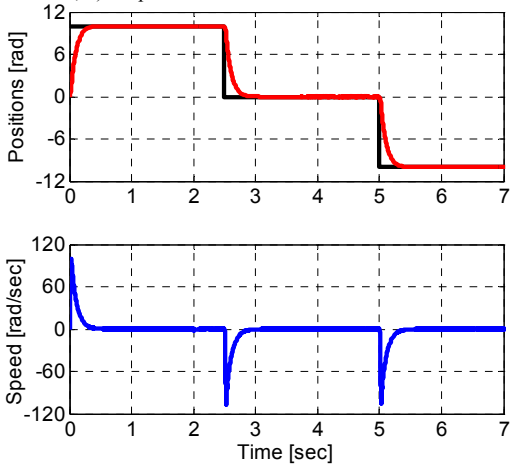

Figure 7. The simulation results showing the tracking performance of the proposed adaptive sliding mode position controller under a step position reference change in forward and reverse directions with load torque of 2 Nm

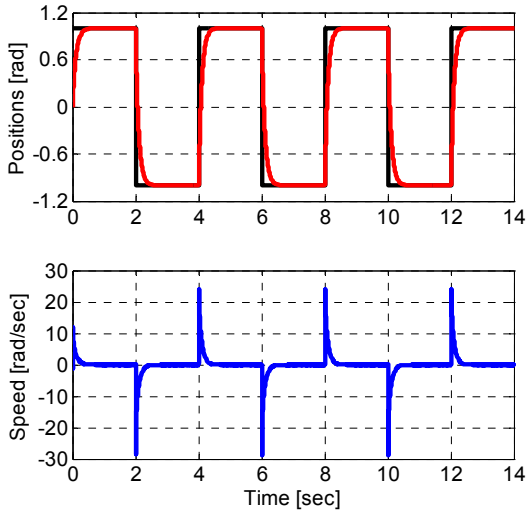

Figure 8. The simulation results showing the tracking performance under a square wave trajectory at position reference changed from 1 to −1 rad with load torque 2 Nm

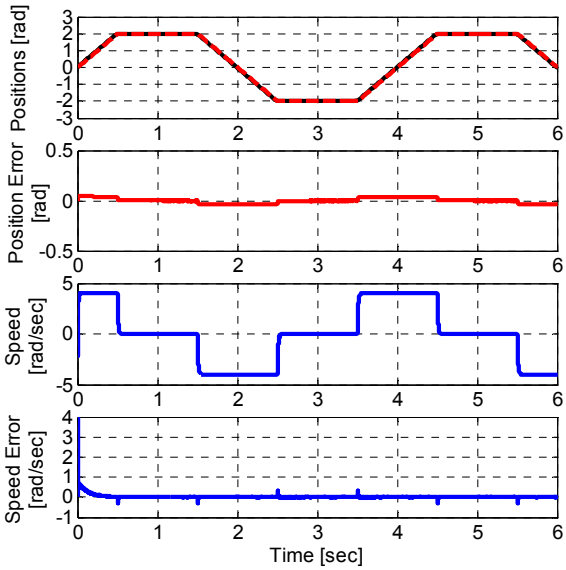

Figure 9. The simulation results showing the tracking performance of the proposed adaptive sliding mode position controller under a trapezoidal position reference of 2 rad with load torque of 2 Nm

VI. Experimental Results

A. Real-Time Implementation of the Drive System

In order to verify the effectiveness of the proposed position controller based IPMSM, the experimental implementation of the control scheme is carried out according to Fig. 12. The experimental setup incorporates a DSP control board DS1102, which is based on a 32-bit floating point DSP TMS320C31. The IPMSM is coupled with a separately excited DC generator for loading. The IPMSM is supplied by a three-phase voltage-source Pulse Width Modulated (PWM) inverter, which is composed of six IGBT's and a gate driver board. The inverter used in the experimental system is POWEREX Module (PM25RSB120) 25 Amperes/1200 Volts. Two phase currents i_a and i_b are sensed by Hall-effect current sensors (LA 25-NP). These currents are fed to the DSP board through the analog-to-digital converter. The third phase current is computed in software program inside DSP control board. Also, the position of the rotor is sensed by an incremental encoder and fed to the encoder interface on the DSP board. The encoder

generates 2048 pulses per revolution.

Hysteresis controller is used for current control and producing gate pulses. These pulses are six logic signals, which are sent to the inverter via digital Input/Output (I/O) ports and isolation gate drive circuit.

B. Experimental Responses

The experimental results to show the performance of the position controller are presented as shown in Fig. 13. The actual position tracks the reference one smoothly using the proposed controller. Thus, a good position tracking has been achieved for the proposed adaptive gain SMC, which is not the case with the fixed feedback gain SMC-controller-based drive system.

The experimental position and speed responses to verify the validity of the proposed controller under load torque disturbances is presented in Fig. 14. In this figure, the rotor position tracks the desired reference position in spite of load torque disturbances. There is a sudden load torque of 2 Nm at $t = 1$ sec. As shown, a small position error can be noted at this time $t = 1$ sec. However, the rotor position error is removed after a short time because of the adaptive feedback gain. It is observed that a good load torque rejection is achieved. This confirms that the proposed SM position control scheme works properly.

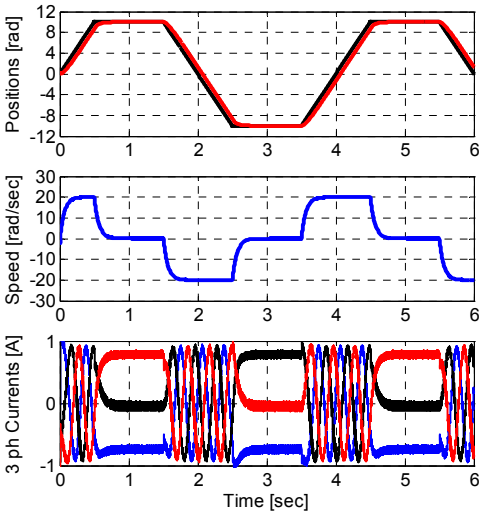

Figure 10. The simulation results showing the performance of the proposed adaptive sliding mode position controller under applying a trapezoidal reference tracking at a position reference of 10 rad with load torque of 2 Nm

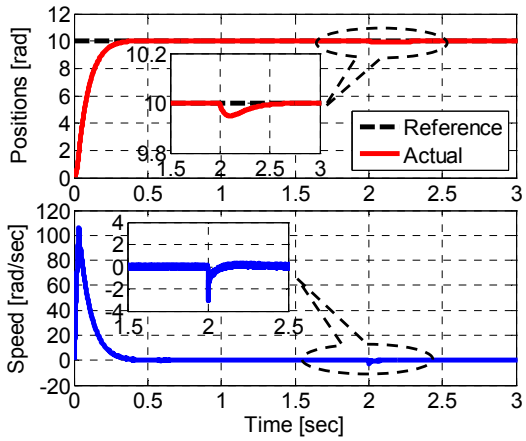

Figure 11. The simulation results showing the performance of the proposed adaptive sliding mode position controller under load torque disturbance of 2 Nm applied at 2 sec using a position reference of 10 rad

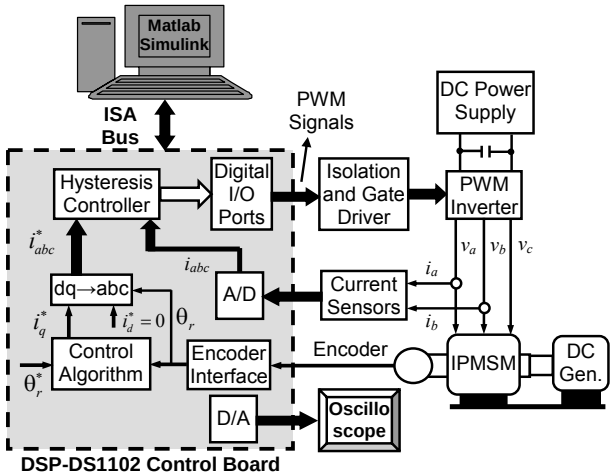

Figure 12. Block diagram of DSP-based real- time implementation of control algorithms for IPMSM drive system

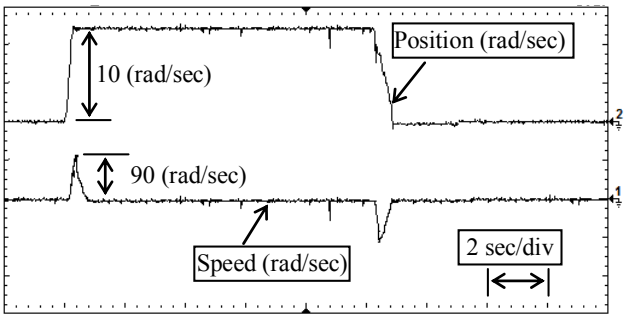

Figure 13. Experimental position responses showing the performance of the proposed adaptive sliding mode position controller under applying a trapezoidal reference tracking at a position reference of 10 rad with a load torque of 2 Nm

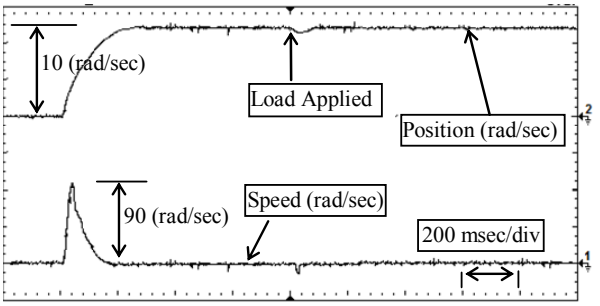

Figure 14. Experimental position responses using the proposed adaptive sliding mode position controller under starting and sudden load application of 2 Nm applied at 2 sec at a position reference of 10 rad.

VII. Conclusion

In this paper, an adaptive and robust sliding mode position control of an IPMSM drive has been proposed. The switching surface of SMC has been designed using a LQR technique. The quadratic optimal control method has been used to select the state feedback control gain. Feedback and switching gains are selected to satisfy both stability and fast convergence of the IPMSM. Simulation and experimental results have been presented to validate the performance of the position control method. A SMC-based IPMSM drive system with adaptive feedback gain design has confirmed a superior behavior than a traditional SMC. As proved, the conventional SMC is sensitive to parameters uncertainty in the reaching mode. However, the proposed SMC position controller has no overshoot with a less sensitivity to parameters uncertainty. Also, the rotor position is robust to a load disturbance and backs rapidly without chattering.

APPENDIX

TABLE I. INTERIOR PERMANENT MAGNET SYNCHRONOUS MOTOR PARAMETERS

Rated power (HP)	1	R_s	10.5 Ohm
Phase voltage (Volt)	220	L_d	159 mH
Phase current (Amp.)	1.6	L_q	245 mH
Rated Speed (rpm)	1500	λ_m	0.756 V.S/Rad
Number of poles	4	J_o	0.003 Kg.m^2

ACKNOWLEDGMENT

The authors would like to thank the reviewers for their professional work and helpful suggestions.

REFERENCES

[1] M.A. Rahman, M.A. Masrur, M.N. Uddin, "Impacts of Interior Permanent Magnet Machine Technology for Electric Vehicles," IEEE International Electric Vehicle Conference (IEVC), Greenville, SC, 4-8 March 2012, pp. 1-5. doi: 10.1109/IEVC.2012.6183226

[2] M.N. Uddin, T.S. Radwan, M.A. Rahman, "Performance of interior permanent magnet motor drive over wide speed range," IEEE Trans. Energy Convers., vol, 17, no. 1, pp. 79–84, 2002. doi: 10.1109/60.986441

[3] M.S. Zaky, M.A. Hassanien, S.S. Shokralla, "high dynamic performance of IPMSM Drives based on Feedforward Load Torque Compensator," Electric Power Components and Systems, vol. 41, no. 3, pp. 235–251, 2013. doi:10.1080/15325008.2012.742940

[4] M.S. Zaky, "A self-tuning PI controller for the speed control of electrical motor drives," Electric Power Systems Research, Elsevier, vol. 119, pp. 293–303, 2015. doi:10.1016/j.epsr.2014.10.004

[5] R. Shahnazi, H.M. Shanechi,, N. Pariz, "Position Control of Induction and DC Servomotors: A Novel Adaptive Fuzzy PI Sliding Mode Control," IEEE Transactions on Energy Conversion, vol. 23, no. 1, pp.138-147, 2008. doi: 10.1109/TEC.2007.905070

[6] F. Betin, D. Pinchon, G.A. Capolino, A time-varying sliding surface for robust position control of a DC motor drive, IEEE Trans. on Ind. Electron., vol. 49, no. 2, pp. 462-473, 2002. doi: 10.1109/41.993280

[7] K.V. Prashanth, H.G. Navada, "Position Control of Interior Permanent Magnet Synchronous Motor using Adaptive Backstepping Technique," IEEE International Conference on Advances in Computing, Communications and Informatics (ICACCI), Mysore, pp. 1718-1723, 22-25 Aug. 2013. doi: 10.1109/ICACCI.2013.6637440

[8] Y. Seki, K. Ohishi, Y. Yokokura, M. Matsuhashi, T. Mashimo, "High-speed Position Control of SPMSM using Rapid Current Profiling Technique Based on Angular Impulse," 13th IEEE International Workshop on Advanced Motion Control (AMC, Yokohama, pp. 512-517), 14-16 March 2014. doi: 10.1109/AMC.2014.6823334

[9] P. Alkorta, O. Barambones, F.J. Vicandi, J.A. Cortajarena, I. Martija, "Effective Proportional Derivative position control of induction motor drives," IEEE International Conference on Industrial Technology (ICIT), 14-17 March 2016, Taipei, Taiwan, pp. 147 – 152. doi: 10.1109/ICIT.2016.7474741

[10] A.B. Junior, T.R. Neto, D.A. Honório; L.H. Barreto, L.N. Reis, "Hybrid Position Controller for an Indirect Field-Oriented Induction Motor Drive," IEEE Applied Power Electronics Conference and Exposition (APEC), Charlotte, North Carolina, 15-19 March 2015, pp. 1541 -1547. doi: 10.1109/APEC.2015.7104552

[11] C.K. Lin, T.H. Liu, S.H. Yang, "Nonlinear position controller design with input–output linearisation technique for an interior permanent magnet synchronous motor control system," IET Power Electron., vol. 1, no. 1, pp. 14–26, 2008. doi: 10.1049/iet-pel:20070177

[12] C. K. Lai, K. K. Shyu, "A Novel Motor Drive Design for Incremental Motion System via Sliding-Mode Control Method," IEEE Trans. on Ind. Electron., vol. 52, no. 2, pp. 499-507, 2005. doi: 10.1109/TIE.2005.844230

[13] M.A. Rahman, M.A. Hoque, "On-line adaptive artificial neural network based vector control of permanent magnet synchronous motors," IEEE Trans. Energy Convers., vol. 13, no. 4, pp. 311-318, 1998. doi: 10.1109/60.736315

[14] M.N. Uddin, M.A. Abido, M.A. Rahman, "Development and implementation of a hybrid intelligent controller for interior permanent-magnet synchronous motor drives," IEEE Trans. Ind. Appl., vol. 40, no. 1, pp. 68-76, 2004. doi: 10.1109/TIA.2003.821797

[15] M.N. Uddin, T.S. Radwan, M.A. Rahman, "Fuzzy-logic-controller-based cost-effective four-switch three-phase inverter-fed IPM synchronous motor drive system," IEEE Trans. Ind. Appl., vol. 42, no. 1, pp. 21-30, 2006. doi: 10.1109/TIA.2005.861277

[16] M.N. Uddin, Z.R. Huang, A.B. Hossain, "Development and Implementation of a Simplified Self-Tuned Neuro–Fuzzy-Based IM Drive," IEEE Trans. on Ind. Appl., vol. 50, no. 1, pp. 51- 59, 2014. doi: 10.1109/TIA.2013.2269131

[17] R.S. Rebeiro, M.N. Uddin, "FLC based tuned PI controller for wide speed range operation of IPMSM drive," IEEE Power and Energy Society General Meeting, pp. 1-5, 25-29 July 2010. doi: 10.1109/PES.2010.5589714

[18] B. Veselic, B.P. Drazenovic, C. Milosavljevic, "High-Performance Position Control of Induction Motor Using Discrete-Time Sliding-Mode Control," IEEE Trans. on Ind. Electron., vol. 55, no. 11, pp. 3809-3817, 2008. doi: 10.1109/TIE.2008.2006014

[19] K.K. Shyu, C.K. Lai, Y.W. Tsai, D.I. Yang, "A newly robust controller design for the position control of permanent-magnet synchronous motor," IEEE Trans. on Ind. Electron., vol. 49, no. 3, pp. 558- 565, 2002. doi: 10.1109/TIE.2002.1005380

[20] A. Saghafinia, H.W. Ping, M.N. Uddin, K.S. Gaeid, "Adaptive Fuzzy Sliding-Mode Control Into Chattering-Free IM Drive," IEEE Trans. on Ind. Appl., vol. 51, no. 1, pp. 692- 701, 2015. doi: 10.1109/TIA.2014.2328711

[21] O. Barambones, "An Adaptive Robust Position Control for Induction Machines using a Sliding Mode Flux Observer," 9th IEEE International Symposium on Diagnostics for Electric Machines, Power Electronics and Drives (SDEMPED), Valencia, pp. 439-446, 27-30 Aug. 2013. doi: 10.1109/DEMPED.2013.6645753

[22] C.M. Liaw, Y.M. Lin, K.H. Chao, "A VSS speed controller with model reference response for induction motor drive," IEEE Trans. Ind. Electron., vol. 48, no. 6, pp. 1136–1147, 2001. doi: 10.1109/41.969392

[23] F.J. Lin, K.K. Shyu, Y.S. Lin, "Variable structure adaptive control for PM synchronous servo motor drive," IEE Proc Elect Power Appl., vol. 146, no. 2, pp. 173–185, 1999. doi: 10.1049/ip-epa:19990113

[24] S.K. Chung, J.H. Lee, J.S. Ko, M.J. Youn, "Robust speed control of brushless direct-drive motor using integral variable structure control," IEE Proc. Elect. Power Appl., vol. 142, no. 6, pp. 361–370, 1995. doi: 10.1049/ip-epa:19952230

[25] K.C. Hsu, H.H. Chiang, C.I. Huang, T.T. Lee, "Optimized adaptive sliding-mode position control system for linear induction motor drive," 10th IEEE International Conference on Networking, Sensing and Control (ICNSC), 10-12 April 2013, pp. 355 - 360. doi: 10.1109/ICNSC.2013.6548763

[26] O. Barambones, and P. Alkorta, "Position control of the induction motor using an adaptive sliding-mode controller and observers," IEEE Trans. on Ind. Electron., vol. 61, no. 12, 2014, pp. 6556-6565. doi: 10.1109/TIE.2014.2316239

[27] O. Barambones, P. Alkorta, J.M. Durana, "Adaptive sliding mode position control for electrical motors," International Conference on Computational Science and Computational Intelligence, Las Vegas, Nevada, USA, 10-13 March 2014, vol. 2, pp. 17 - 23. doi: 10.1109/CSCI.2014.88

[28] F. Betin; G.A. Capolino, "Sliding mode control for electrical drives," IEEE International Electric Machines & Drives Conference (IEMDC), Coeur d'Alene, ID, USA, 10-13 May 2015, pp. 1043-1048, doi: 10.1109/IEMDC.2015.7409190

[29] M.S. Zaky, "Robust chatter-free continuous VSC for the speed control of electrical motor drives using adaptive feedback gain," Electric Power Systems Research, Elsevier, vol. 140C, pp. 786-796, 2016. doi: 10.1016/j.epsr.2016.05.007

[30] P.A. Egiguren, O.B. Caramazana, "Robust Position Control of Induction Motor Drives," IEEE International Symposium on Industrial Electronics (ISIE), Bari, Italy, 4-7 July 2010, pp. 1468-1473. doi: 10.1109/ISIE.2010.5637877